AN OBSTACLE AVOIDANCE ALGORITHM FOR A CAR PULLING MANY TRAILERS WITH KINGPIN HITCHING

by

Anant Sahai, Matthew Secor, and Linda Bushnell

Memorandum No. UCB/ERL M94/10

3 March 1994

AN OBSTACLE AVOIDANCE ALGORITHM FOR A CAR PULLING MANY TRAILERS WITH KINGPIN HITCHING

by

Anant Sahai, Matthew Secor, and Linda Bushnell

Memorandum No. UCB/ERL M94/10

3 March 1994

ELECTRONICS RESEARCH LABORATORY

College of Engineering
University of California, Berkeley
94720

[1]A. Sahai and M. Secor were both supported by NSF REU grant IRI-9014490. L. Bushnell was supported in part by NSF under grant IRI-9014490. Please send all correspondences to L. Bushnell at the above address. A version of this paper was submitted to the 33rd IEEE CDC.

Abstract

We present a new method for planning motion around obstacles for a mobile robot system configured as a car pulling many trailers with non-standard kingpin hitching. In our method, we need only plan for the front car and the trailers will follow without hitting obstacles. We assume there are no back-ups in the trajectory. By setting the distance between an axle and its neighboring kingpin to be the same for all axles, by showing exponential convergence of the distance between the path followed by a trailer and the path followed by the car, and by showing there exists a bound on this distance, we propose an obstacle avoidance algorithm for a multi-trailer system using any existing path planner for the front car only. Examples are given for a car pulling a single trailer and three trailers.

Keywords: obstacle avoidance, wheeled mobile robots.

Chapter 1

Introduction

One application of obstacle avoidance that motivates this research is automatically controlling a car with many trailers through danger areas such as a nuclear power plant or a mining site. These areas are unsafe for human operators and are a maze of narrow corridors and obstacles. In this report, we are interested in obstacle avoidance for wheeled nonholonomic systems, specifically car-like robots with many trailers [1, 2].

Instead of using axle-to-axle hitching, we consider the more general kingpin hitching where the axles are connected by a kingpin (or kingbolt) between the bodies. Our method for obstacle avoidance uses a particular case of this in which the lengths of the links in the kingpin hitching are equal. We then give an algorithm that need only plan the trajectory for the front car. We give sufficient conditions to guarantee that the trailers avoid the same obstacles as the car. These conditions depend on a "deviation bound" for each trailer, which is defined to be the maximal distance a trailer will swing off the front car's track when the car changes from one path to another. In addition, we prove exponential convergence of the trailer approaching its steady-state circular path when the front car is on a circular path.

The outline of the paper is as follows: in Chapter 2, we present some relevant background information for the obstacle avoidance problem. In Chapter 3, we describe in detail our obstacle avoidance algorithm. In Chapter 4, we give examples of a car pulling one trailer and a multi-trailer mobile robot system to illustrate our algorithm. In Chapter 5, conclusions are made.

Chapter 2

Background

A good recent review of nonholonomic motion planning is [3]. For example, [4] discusses the problem of planning smooth paths for a mobile robot with a minimum turning radius. Collision-free subpaths that go between points on the obstacle boundaries are first computed, then the subpaths are smoothly concatenated into the final path.

Controllability of an n-body mobile robot system with the standard axle-to-axle hitching is proven in [5]. Controllability of a two-body mobile robot system with the non-standard kingpin hitching is shown in [6]. In this same reference, the nonholonomic path planning problem for mobile robots is solved by first using a general geometric planning algorithm to find a path without accounting for the nonholonomic constraints of the controllable system. These algorithms are solutions to the classical Piano Mover problem. In the second step, the system is steered along an admissible collision-free path as near to the first path, taking into account the nonholonomic constraints.

In [7], a fast and exact motion planner is presented for a mobile robot with a bounded turning radius. Again, a general path planning algorithm is used to compute a collision-free path. The path is then transformed into one which obeys the nonholonomic and curvature constraints by using subgoals along the initial path. The subpaths are concatenated to make the final path, which is then optimized for near-minimal length.

In general geometric planning algorithms [8] using a configuration space formulation, the procedure to plan a path for a car with multiple trailers would be to enclose

the whole mobile robot in one circle and use this circle to "grow" the obstacles in the robot's configuration space. The collision-free path for this "point robot" is then planned in the configuration space. Using this method, the planned trajectory would be far away from all obstacles since the resulting highway would be wide. As will be seen in the next chapter, our method greatly reduces this distance, allowing for more agile maneuverability.

In [9], the shortest paths between any two configurations for a two-axle vehicle are completely characterized. The path is allowed to have cusps, or reversals. We are not concerned with shortest paths in this paper, however, and only deal with paths that have no back-ups. This is analogous to the seminal paper by Dubins [10] in which the shortest obstacle-free paths are derived for a system similar to a car-like robot. The velocity of the system is held constant and no cusps are allowed in the path; it is only made up of straight line segments and arcs of circles.

Chapter 3

Obstacle Avoidance Algorithm

The algorithm described in this chapter was inspired from experience we received using an interactive steering software program that we developed on a SiliconGraphics workstation. For a detailed description including software code, please refer to [11].

In this chapter, we consider in detail a car with one trailer with the non-standard kingpin hitching as shown in Figure 3.1. The body angles of the car and trailer are denoted by θ_0 and θ_1, respectively. We denote the distance from the center of the car's (trailer's) axle to the kingpin as L_1 (L_2).

The main idea of the algorithm is to grow the obstacles in the configuration space of the mobile robot using a circle around the front car (assuming it has the largest body) increased by a "trailer correction factor," which depends on bounds that will be computed in this chapter. The resulting circle is represented as a "point robot" for which an obstacle-free trajectory can be planned using an existing path planner.

We make one assumption for our algorithm: no back-ups are allowed. At this time, our algorithm does not handle trajectories with back-ups; we only consider paths made of straight line segments and arcs of circles as in [10]. We will show that

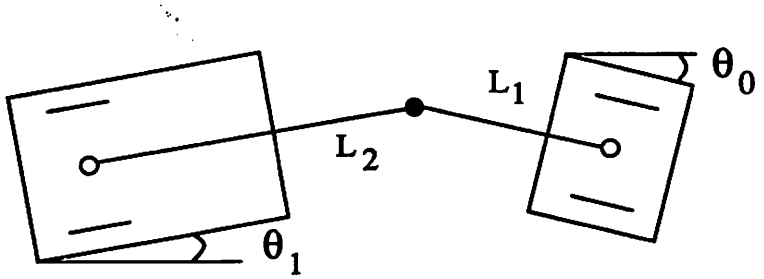

Figure 3.1: A car with one trailer with kingpin hitching.

the trailers do not stray too far away from the path of the front car and eventually converge to this path. Below we will prove three theorems that quantify this idea for the case of a car pulling one trailer (a two-axle system). The theorems can be easily extended for a car with more than one trailer by making all of the subsequent calculations for the last trailer in the convoy. Exponential convergence to a circle (for straight line, we consider the radius to be infinity) is proven and bounds are found on the amount the trailer strays away from the car's path for two special cases:

1. The transition from a straight line to an arc of a circle of radius r.
2. The transition from an arc of a circle of radius r to a straight line.

In the following, we use "path of the car" or "path of the trailer" to mean the trajectory of the center of the axle.

Theorem 1 *If the front car in a two-axle system follows a circular path (a straight line is considered a circle with an infinite radius), then the trailer approaches a circular path. These circular paths have the same center. Furthermore, the convergence of the trailer to its steady-state circular path is exponential in distance traveled.*

Proof. The proof refers to Figure 3.2 and is only concerned with axle-to-axle hitching. We will show that $\tilde{r}$, defined as the distance of the segment from B to C, converges to some fixed value which we will denote $\hat{r}$. This will show that the path of the trailer does indeed converge to a circle. We begin by giving an expression for $\tilde{r}$. To do this we assign coordinates to the system as shown in Figure 3.2. We assign the origin to A, the location of the center of the car's axle, and let the positive x axis run along the line from A to some point D, such that ADC is a right triangle as in the figure. Then we see that the Cartesian coordinates of the points B and C are

$$\begin{aligned} B &= (\ell_2 \cos\phi, \ell_2 \sin\phi) \\ C &= (\ell_1, -r) \ . \end{aligned}$$

Using the normal Euclidean distance function we get

$$\tilde{r} = \sqrt{(\ell_2 \cos\phi - \ell_1)^2 + (\ell_2 \sin\phi + r)^2} \ . \tag{3.1}$$

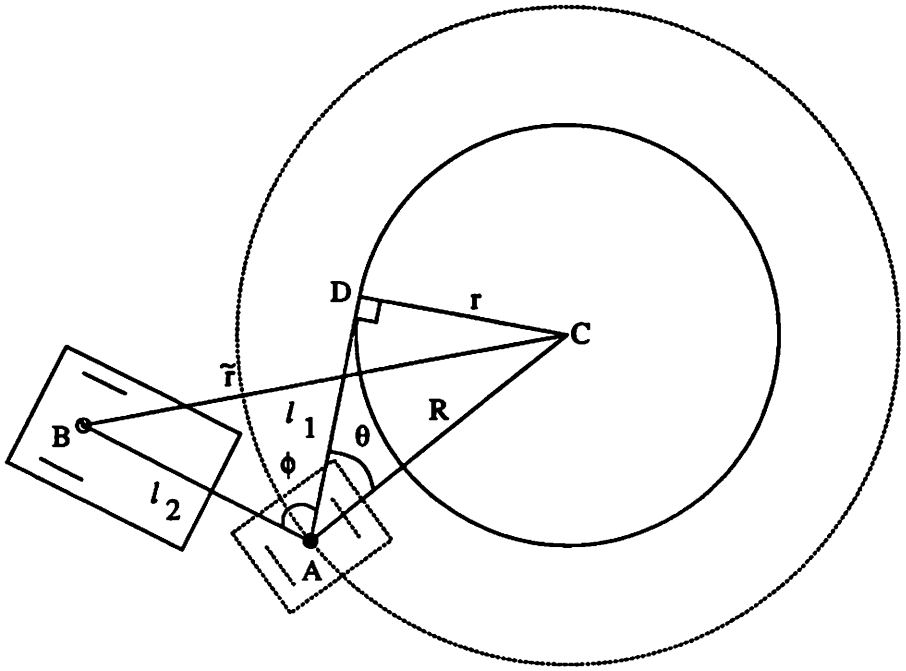

Figure 3.2: For axle-to-axle hitching, the front car is traveling along a circle of radius R. The trailer is shown to converge to a circle of radius r.

We take the partial derivative with respect to ℓ_2, since that is the direction in which the back trailer moves. Since our original choice of placing point D was arbitrary, we can let $L := \ell_1 = \ell_2$ to get

$$\frac{\partial \tilde{r}}{\partial \ell_2} = \frac{L}{\tilde{r}} \left(1 - \cos\phi + \frac{r}{L} \sin\phi\right) . \tag{3.2}$$

By using law of cosines on the triangle ABC, we see that

$$\cos(\theta + \phi) = \frac{L^2 + R^2 - \tilde{r}^2}{2LR} .$$

Since ADC is a right triangle we have

$$\begin{aligned} \cos\theta &= \frac{L}{R} \\ \sin\theta &= \frac{r}{R} , \end{aligned}$$

and by using the cosine addition formula we have

$$L\cos\phi - r\sin\phi = \frac{L^2 + R^2 - \tilde{r}^2}{2L} . \tag{3.3}$$

Substituting (3.3) into (3.2) we get

$$\frac{\partial \tilde{r}}{\partial \ell_2} = \frac{L}{\tilde{r}} \left(1 - \frac{L^2 + R^2 - \tilde{r}^2}{2L^2}\right) ,$$

and simplifying we have

$$\frac{\partial \tilde{r}}{\partial \ell_2} = \left(\frac{L^2 - R^2 + \tilde{r}^2}{2L\tilde{r}} \right) .$$

By using the fact that $r^2 = R^2 - L^2$, we see

$$\frac{\partial \tilde{r}}{\partial \ell_2} = \left(\frac{\tilde{r}^2 - r^2}{2L\tilde{r}} \right) ,$$

which makes it clear that $\tilde{r}$ does indeed tend to r. Therefore, $\hat{r} = r$. To see the rate of convergence more clearly, we let $y = \tilde{r} - r$ so that

$$\frac{\partial y}{\partial \ell_2} = \frac{\partial \tilde{r}}{\partial \ell_2} = \left(\frac{2y\tilde{r} - y^2}{2L\tilde{r}} \right) ,$$

and simplify to get

$$\frac{\partial y}{\partial \ell_2} = \frac{y}{L} - \frac{y^2}{2L\,(r+y)} . \tag{3.4}$$

As we are assuming that the cars are being driven forward, let s be the distance traveled by the back trailer. Since a positive ds implies a negative $d\ell_2$, we have

$$\frac{dy}{ds} = -\frac{y}{L} + \frac{y^2}{2L\,(r+y)} . \tag{3.5}$$

Let y_0 be the initial condition for y, i.e., the value for y just as the front car begins to move on the given circle. To bound y as a function of s, we notice that if $y_0 < 0$ then the second term of equation (3.5) can be dropped to yield

$$y(s) \leq y_0 e^{-\frac{s}{L}} . \tag{3.6}$$

If $y_0 > 0$, we can substitute y_0 for y in the second term of equation (3.5) and thus show that

$$y(s) \leq y_0 \ \exp\left(-\left(\frac{2r + y_0}{2L(r+y_0)} \right) s \right) . \tag{3.7}$$

With these two inequalities, we can conclude exponential convergence of the back trailer to a circle of radius r where

$$r = \sqrt{R^2 - L^2} \tag{3.8}$$

as long as $R > L$.

We now consider the case of a two-axle system with kingpin hitching as shown in Figure 3.1. By the above arguments the we can state the following corollary which shows us what is special about the case $L_1 = L_2$.

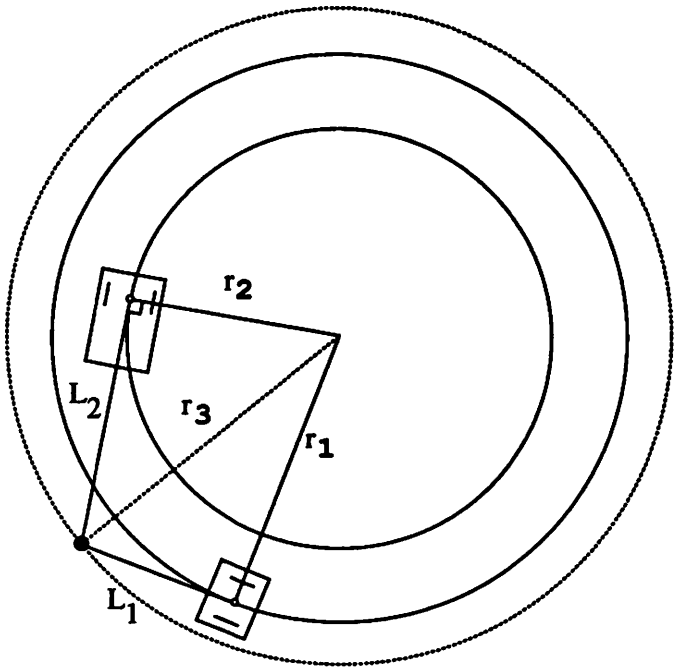

Figure 3.3: For kingpin hitching, the front car is traveling along a circle of radius r_1. The trailer is shown to converge to a circle of radius r_2.

Corollary 1 *Consider a two-axle system with kingpin hitching of lengths L_1 and L_2. If the front car travels along a path of radius r_1, then the trailer will converge to a circle of radius of r_2 where*

$$r_2 = \sqrt{{r_1}^2 + {L_1}^2 - {L_2}^2} \tag{3.9}$$

provided that the expression in (3.9) is well defined.

Proof. We use the result from the previous theorem. We are concerned with the trajectories of the three points: the centers of the axles and the kingpin hitch. Since the front car moves along a circle of radius r_1, the kingpin hitch travels along a circle of some radius r_3 as shown in Figure 3.3. We know by the Pythagorean theorem that

$$r_3 = \sqrt{r_1^2 + L_1^2}\ .$$

We note that the system of the kingpin hitch and the trailer is the same as the system in Theorem 1. Therefore, setting $R = r_3$, by equation (3.8) we have

$$r_2 = \sqrt{r_3^2 - {L_2}^2}\ .$$

These two equations combined give us equation (3.9).

In particular, when $L_1 = L_2$ we see by equation (3.9) that the trailer converges to the same circle as the car.

We now assume that $L := L_1 = L_2$ and compute bounds on the distance the trailer is away from the trajectory of the car when it changes from a straight line to an arc of a circle with radius r. We know by (3.9) that $r_1 = r_2 = r$ and so we expect the deviation to be small.

Theorem 2 *Consider a two-axle system with $L := L_1 = L_2$. If the front car moves from a straight line path to one which is an arc of a circle of radius r, then an upper bound on the distance between the path followed by the trailer and the path followed by the car, z, is*

$$z(s) \leq \begin{cases} y_0 \exp\left(-\left(\frac{2r+y_0}{2L(r+y_0)}\right)s\right) + r - \sqrt{(2L-s)^2 + r^2} & \text{for } 0 \leq s \leq 2L \\ y_0 \exp\left(-\left(\frac{2r+y_0}{2L(r+y_0)}\right)s\right) & \text{for } s > 2L \end{cases} \tag{3.10}$$

where y_0 is the initial distance of the trailer from the car and is given by

$$y_0 = \sqrt{4L^2 + r^2} - r \ , \tag{3.11}$$

and s is the distance traveled by the trailer from when the car switched onto the new circle.

Proof. The proof refers to Figure 3.4. We assume the car travels from point A to point D along a straight line, then at D, switches to the arc of a circle of radius r.

By simple trigonometry, we see that y_0 as defined in (3.11) is correct.

We first want to find a bound on the distance z of the path of the trailer from the straight line segment AD (of length $2L$) that connects to the circle that the car moves on. To get the top expression in equation (3.10) for $0 \leq s \leq 2L$, we approximate z by noting that (look at the zoom-up in Figure 3.4)

$$z(s) \leq y(s) - g(s) \ , \tag{3.12}$$

where $g(s)$ is defined as the distance from the circle to point G and $y(s)$ is from equation (3.7). Point G approximates the projection of B onto the line and has Cartesian coordinates given by

$$G = (-(2L - s), r)$$

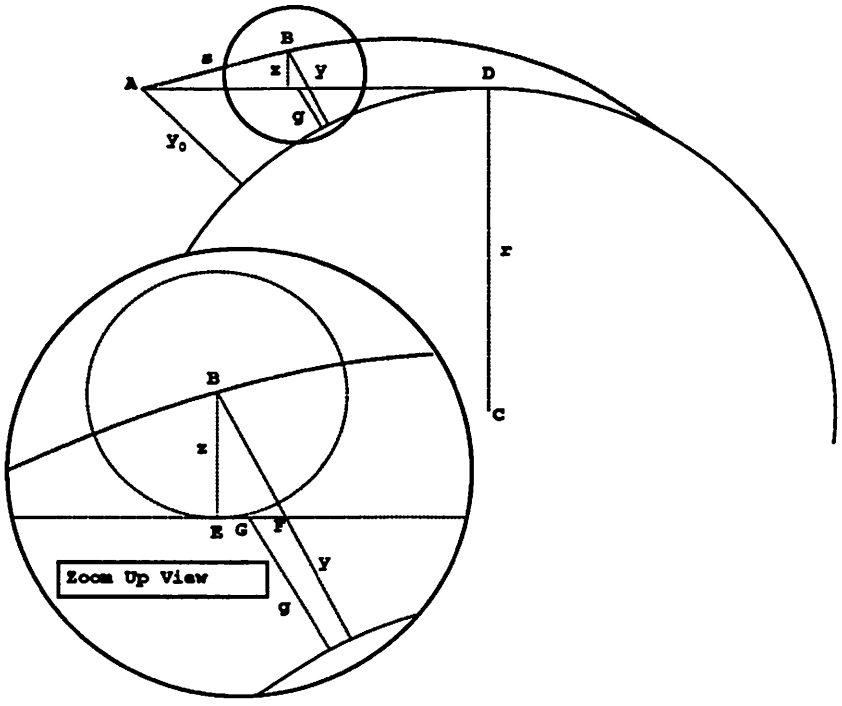

Figure 3.4: Bounds on the trailer when the front car changes its path from a straight line (A to D) to an arc of a circle of radius r. The vehicle is traveling left to right.

with the origin at point C. To get an expression for $g(s)$ we use the normal Euclidean distance function to obtain

$$g(s) = \sqrt{(2L - s)^2 + r^2} - r \ . \tag{3.13}$$

Thus, by combining equation (3.7) with (3.12) and (3.13), we end up with the top equation in (3.10).

When the trailer has passed point D, we know that $z = y$, the distance of the trailer from the circle that the car is moving along. Thus, we use equation (3.7) to bound z for $s > 2L$. This completes the upper bound (3.10).

We continue assuming that $L := L_1 = L_2$ and compute bounds on the distance the trailer is away from the trajectory of the car when it changes from an arc of a circle with radius r to a straight line.

Theorem 3 *Consider a two-axle system with $L := L_1 = L_2$. If the car moves from a path which is an arc of a circle of radius r to a straight line, then an upper bound*

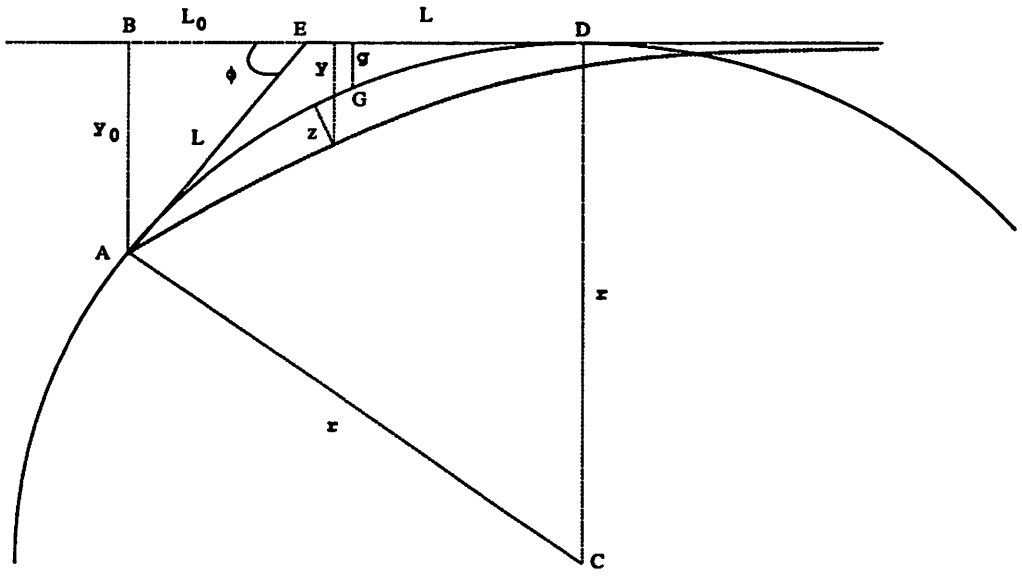

Figure 3.5: Bounds on the trailer when front car changes its path from an arc of a circle of radius r to a straight line. The vehicle is traveling left to right.

on the distance between the path followed by the trailer and the path followed by the car, z, is

$$z(s) \leq \begin{cases} y_0 \exp\left(-\frac{s}{L}\right) + \sqrt{r^2 - (L + L_0 - s)^2} - r & \text{for } 0 \leq s \leq L + L_0 \\ y_0 \exp\left(-\frac{s}{L}\right) & \text{for } s > L + L_0 \end{cases} \tag{3.14}$$

where s is the distance traveled by the trailer from when the car switched to a straight line, y_0 is the initial distance of the trailer from the line the car is moving on at distance $s = 0$ (line segment AB in Figure 3.5) and is given by

$$y_0 = \frac{2L^2 r}{r^2 + L^2}\,, \tag{3.15}$$

and L_0 is as shown in Figure 3.5 (line segment BE) and is such that

$$L + L_0 = \frac{2Lr^2}{r^2 + L^2}\,. \tag{3.16}$$

Proof. The proof refers to Figure 3.5. We assume the car travels along the arc of the circle then switches to the straight line at D. We will use a method analogous to the one we used for the previous theorem.

To get the top expression of equation (3.14), we first consider the part of the path which lies to the left of point D. Let y be the distance of the trailer from the line that the car is moving along. Our first step is to verify that y_0 as defined in (3.15) and $L + L_0$ as defined in (3.16) are correct. To see this we note that

$$y_0 = L \sin \phi \, . \tag{3.17}$$

To compute $\cos \phi$ we use the fact that

$$\sin \phi \ = \sin \angle DEA.$$

Since

$$\angle DEA = \angle DEC + \angle CEA = 2\angle DEC \ ,$$

we have

$$\sin \phi = 2 \sin (\angle DEC) \cos (\angle DEC) = 2 \frac{Lr}{L^2 + r^2} \, . \tag{3.18}$$

Combining (3.17) and (3.18), gives us (3.15) as above. Analogous arguments involving $\cos \phi$ lead us to

$$L_0 = L \frac{r^2 - L^2}{r^2 + L^2} \, . \tag{3.19}$$

Applying (3.19) to $L + L_0$ and simplifying yields (3.16) as above. To get a bound on z we notice that (refer to Figure 3.5)

$$z(s) \leq y(s) - g(s) \tag{3.20}$$

where $g(s)$ is defined as the distance from the line BD to the point G. To get an expression for $g(s)$ we use the Pythagorean theorem and subtract off r to obtain

$$g(s) = r - \sqrt{r^2 - (L + L_0 - s)^2} \, . \tag{3.21}$$

Thus, by combining equation (3.6) with (3.20) and (3.21), we end up with the top equation in (3.14).

To get the bound for $s > L + L_0$, we just use equation (3.6) to get a bound on the distance of the trailer from the straight line that the car moves on. The theorem is proved.

We now use the two bounds given by (3.10) and (3.14) to define the "trailer correction factor", τ. This factor is used to grow the obstacles in the configuration space to guarantee that the trailers will not hit any obstacles.

For a two-axle system with minimum turning radius r, hitching set up with $L_1 = L_2 = L$, we have

$$\tau = \max(Y, H) \ , \tag{3.22}$$

where H represents the deviation of the kingpin hitch from the path of the car when it makes a turn of radius r and is given by (see Figure 3.3)

$$H = \sqrt{r^2 + L^2} - r \ .$$

The bound Y is derived by taking the larger of the maximums of the expressions given in (3.10) and (3.14) by setting r to be the minimum turning radius for the front car. Thus Y represents the worst possible deviation of the trailer from the path of the front car over all permissible paths. By defining Y in this way (i.e. not taking into account the time varying nature of the deviation), we choose a reasonably conservative bound for τ.

To compute τ for a car pulling N trailers, we compute the bounds by (3.22) and add in a correction for more than one trailer. We do this by simply multiplying Y by the number of additional trailers, $N - 1$:

$$\tau = (N - 1) \cdot Y + \max(Y, H) \ . \tag{3.23}$$

This linear scaling is justified since the convergence is exponential and we can propagate the bounds backwards in the trailer system.

Our method for obstacle avoidance for a car with multiple trailers can be summarized in the following algorithm. We are assuming equal kingpin hitching.

Algorithm

1. Construct the smallest circle which can enclose the front car (we are assuming that the front car has the widest body; if it does not, we would use the widest trailer's body).

2. Increase this circle by the trailer correction factor, τ, to take into account the fact that there are multiple trailers attached.

3. Grow the obstacles using this new circle so that we can treat the lead car as a point robot.

4. Plan the trajectory (with no back-ups and bounded turning radius) within the resulting highway through the obstacles using your favorite path planner.

By the above discussion, the trailers will also avoid the obstacles encountered by the front car. Simulations of a car pulling one and three trailers will be presented in the next chapter.

Chapter 4

Examples

Using the interactive steering software package that we developed in [11], we were able to get experimental data that supports our theorems. In this chapter, we will illustrate our obstacle avoidance methodology for two different vehicles: a car pulling one trailer and a car pulling three trailers.

We first consider the case of a car with one trailer, which is attached by means of a kingpin hitch with lengths L_1 and L_2 as shown in Figure 3.1. To investigate what happens under different hitching configurations, these lengths will be varied for the three test cases: (a) $L_1 > L_2$, (b) $L_1 = L_2$, and (c) $L_1 = 0$. We drive the vehicle on a trajectory consisting of a sharp right turn of radius $r = 2.0$. The trajectories of the centers of the axles of the car and trailer are plotted. In addition, we plot the deviation of the trailer from the car's path versus the distance traveled by the trailer for each case. We will show that our calculated bounds for case (b) with the symmetric kingpin hitching configuration closely resemble the experimental data.

For case (a) with $L_1 > L_2$ as shown in Figure 4.1, we notice that the path of the trailer swings out and rapidly settles into being a constant distance away from the path of the car. We can compute this distance by first computing the final radius for the trailer using equation (3.9). We find that r_2 comes out to be $\sqrt{6}$. Thus the distance is $\left(\sqrt{6} - 2\right) \approx 0.449$.

For case (b) with the hitch lengths are equal ($L_1 = L_2$) as shown in Figure 4.2, the trailer closely follows the path of the front car. For this case, we were able to compare the experimental data shown on the right in Figure 4.2 with the bounds predicted by Theorems 2 and 3. Figure 4.3 compares the experimental and predicted deviation of

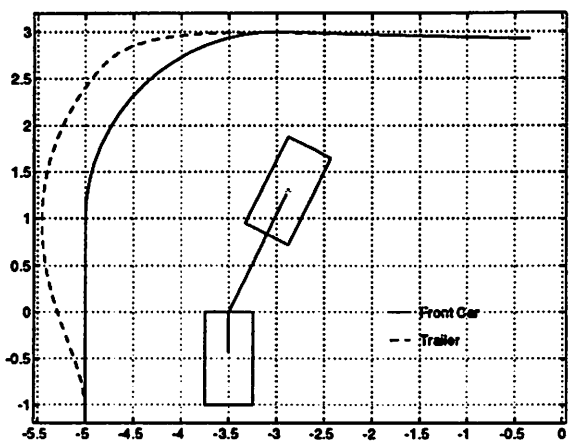

$x - y$ plot of trajectory.

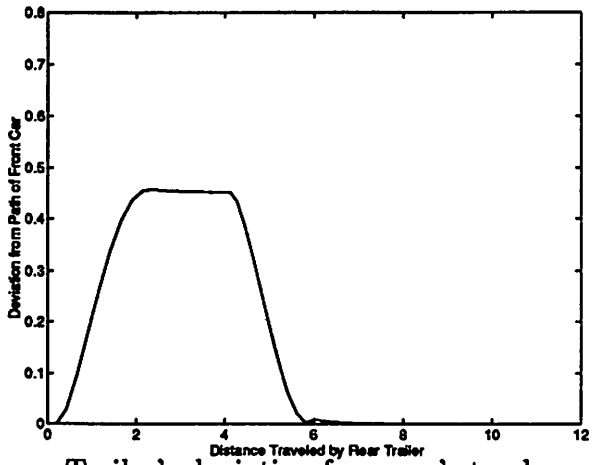

Trailer's deviation from car's track.

Figure 4.1: Case (a): $L_1 = 1.5$, $L_2 = 0.5$. The car (solid line) pulling one trailer (dashed line) with unequal hitch lengths making a right hand turn.

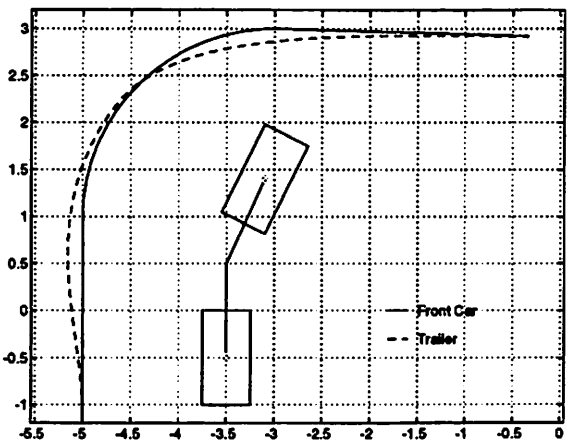

$x - y$ plot of trajectory.

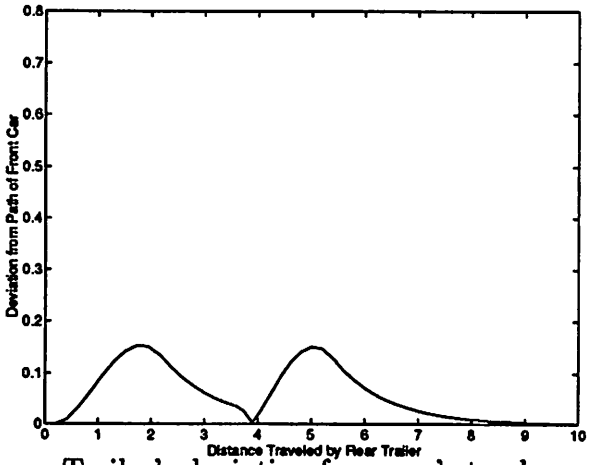

Trailer's deviation from car's track.

Figure 4.2: Case (b): $L_1 = 1.0$, $L_2 = 1.0$. The car (solid line) pulling one trailer (dashed line) with equal hitch lengths making a right hand turn.

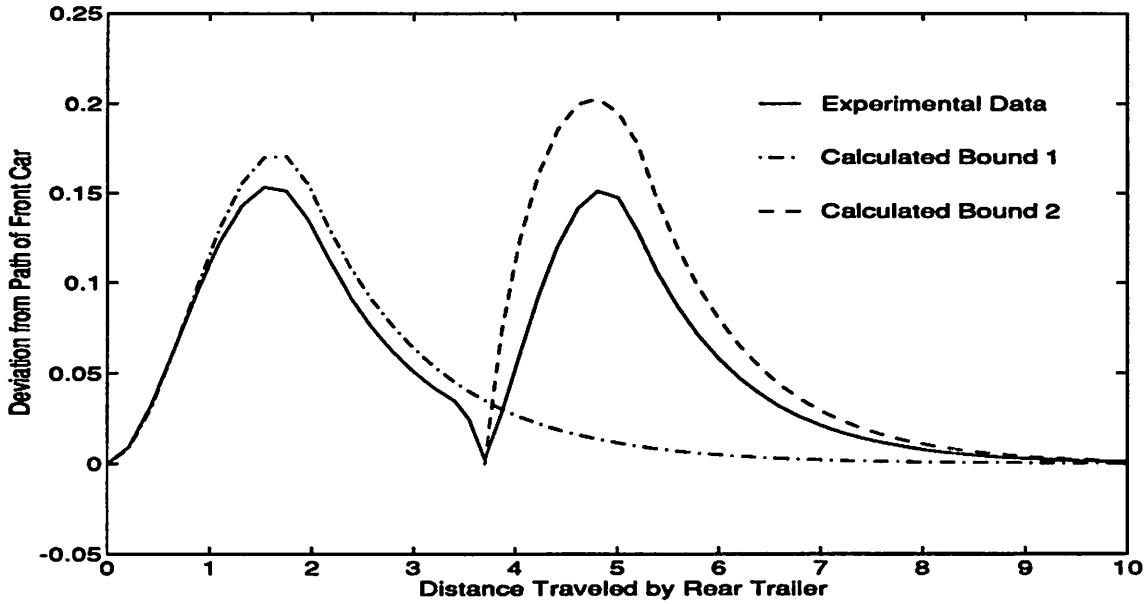

Figure 4.3: Comparison of experimental convergence data with calculated bounds. The trailer system (with $L_1 = L_2 = 1$) is executing the maneuver shown in Figure 4.2.

the trailer from the path of the car. The left hump corresponds to the car changing from a straight line to an arc of a circle. This bound is calculated from equation (3.10). The right hump corresponds to the car changing from an arc of a circle to a straight line and this bound is calculated using equation (3.14). We observe that the second calculated bound is more conservative than the first.

In the third case, shown in Figure 4.4, the first hitch has zero length ($L_1 = 0$). This axle-to-axle hitching configuration is what has been used widely in the literature. We see that the trailer swings in and cuts the corner as compared to the car.

In comparison, we see from these results that with the equal hitching method $L_1 = L_2$, the trailer follows more closely to the lead car's path than with the other two hitching methods.

We next used the interactive software package to drive a car pulling three trailers as shown in Figure 4.5. Figure 4.6 shows the trajectories of the centers of the four axles as the vehicle is driven through an obstacle field. The lengths of all of the hitches were equal and set to 1.0. As the figure indicates, the path swept out by the car and its trailers during motion is not much larger than that of a single car. This

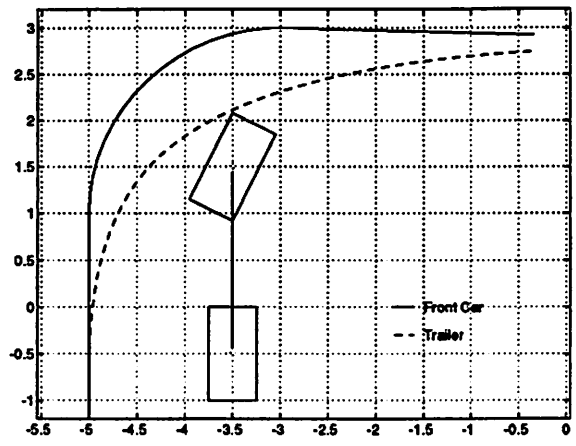

$x - y$ plot of trajectory.

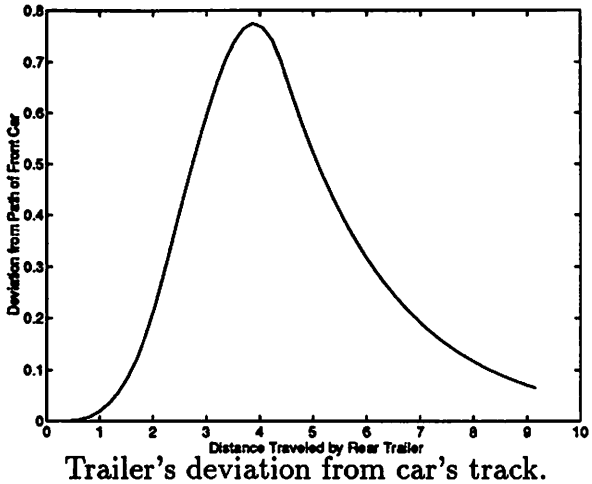

Trailer's deviation from car's track.

Figure 4.4: Case (c): $L_1 = 0.0$, $L_2 = 2.0$. The car (solid line) pulling one trailer (dashed line) with axle-to-axle hitching making a right hand turn.

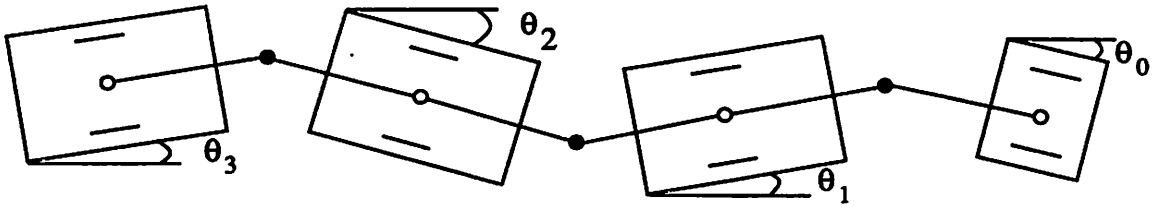

Figure 4.5: Configuration of a car pulling three trailers with kingpin hitching

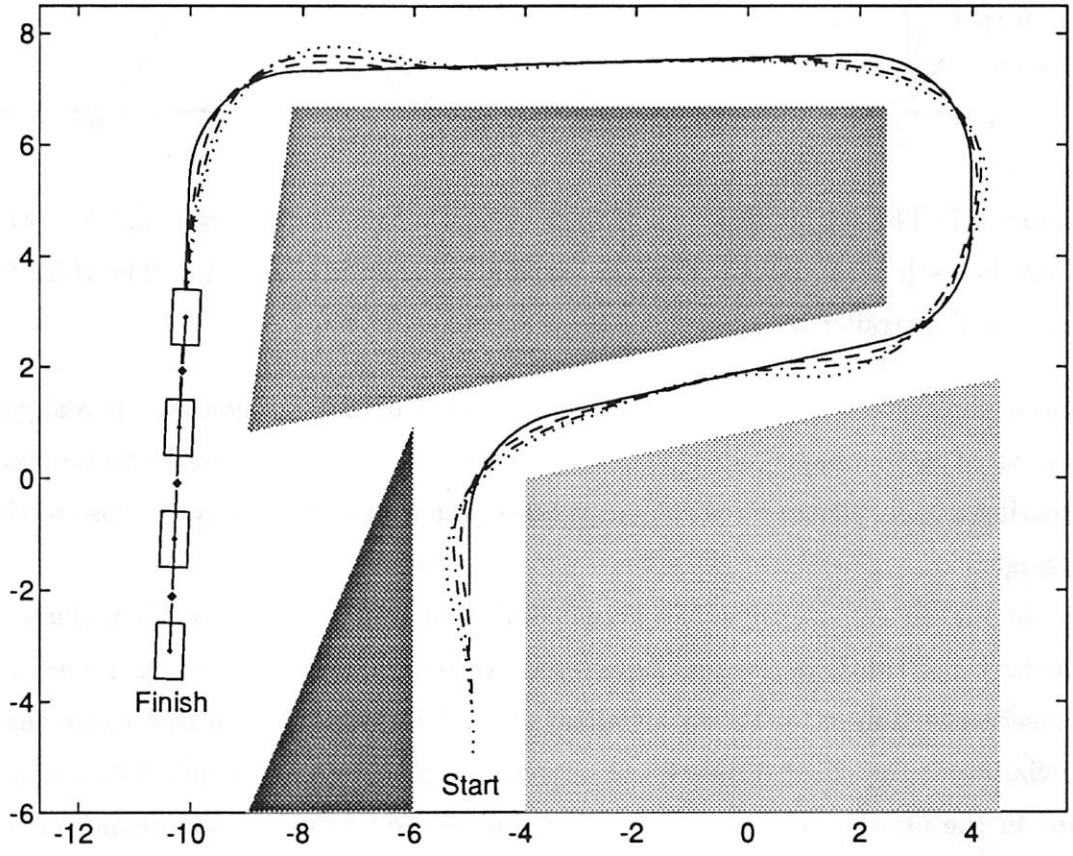

Figure 4.6: Experimental data showing path of a car pulling three trailers through an obstacle field. The front car's trajectory is the solid line.

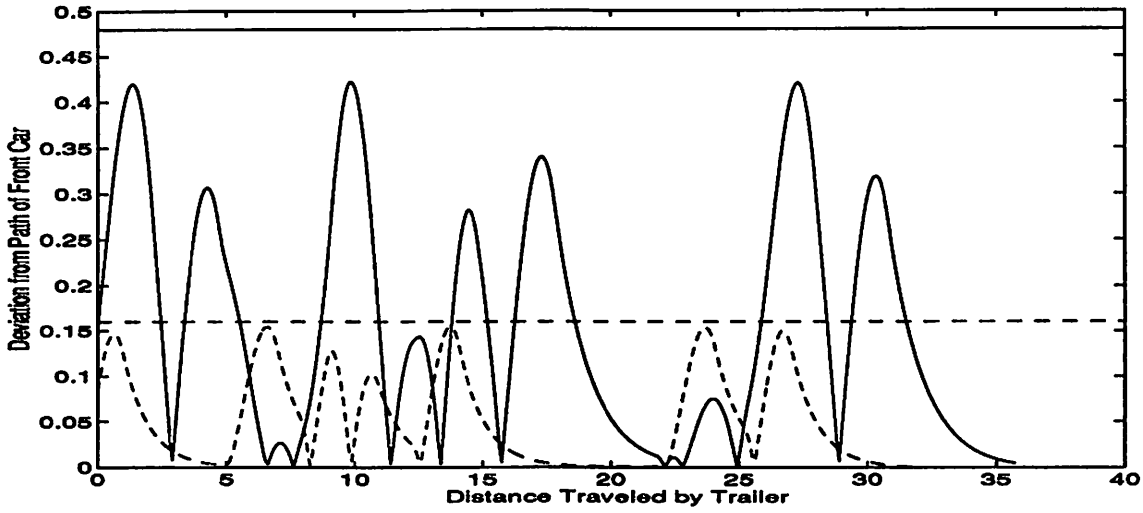

Figure 4.7: The actual deviation of the first (dotted line) and third (solid line) trailers from the path of the front car for the trajectory shown in Figure 4.6. The third trailer lags the first trailer by 4 units.

allows the system to travel quite easily through narrow passageways. The algorithm presented in this paper takes advantage of this fact and allows paths to be planned, treating a multiple-trailered vehicle as an object whose extent is very close to that of a single car.

In Figure 4.7, we show the actual deviation from the front car's trajectory for the first and third trailers for the four-axle system trajectory shown in Figure 4.6. A conservative bound for the first trailer is $Y = 0.16$. We see from this figure that the deviation of the third trailer was less than three times this bound, 0.48 (horizontal line in the figure). This illustrates that linearly adding on a fixed deviation, Y, for each trailer to the trailer correction factor in equation (3.23) is conservative.

Chapter 5

Summary

We have presented a new method for obstacle avoidance for a car with many trailers. By starting with the smallest circle around the front car only, increasing this circle by the "trailer correction factor" defined in this report, and growing the obstacles in the configuration space using this new circle, any existing path planner that avoids back-ups can be used for the resulting point robot. This methodology guarantees that the trailers will also avoid the obstacles. We have thus reduced a difficult problem to a simple methodology.

One inexpensive and practical application of this research is to install flexible "feelers" to the sides of the front car in an multi-trailer system. By adjusting the length of the feelers, if the front car avoids obstacles, the trailers will also avoid the same obstacles. The length of the feelers would be a function of the number of trailers, the radius of curvature of the circle the front car is currently traveling on, and the deviation bounds on the straying of the trailers. Such a set up could then be used to train drivers of cars with many trailers.

Future work includes implementing an existing path planning algorithm using our methodology. We are also interested in exploring the concept of making the trailer correction factor time varying, which would produce more agile trajectories. We plan to extend this research to obstacle avoidance for vehicles with more than one steerable axle such as a fire truck [12] and a multi-steering, multi-trailer vehicle [13, 14].

Acknowledgement

We would like to thank Shankar Sastry for encouraging us in this research endeavor, Gregory Walsh for his insight into the problem and help with the graphical interface, Dawn Tilbury for her helpful comments and simulation data, and John Canny for his helpful discussions.

Bibliography

[1] R. M. Murray and S. S. Sastry, "Nonholonomic motion planning: Steering using sinusoids," *IEEE Transactions on Automatic Control*, pp. 700–716, May 1993.

[2] D. Tilbury, R. Murray, and S. Sastry, "Trajectory generation for the N-trailer problem using Goursat normal form," in *Proceedings of the IEEE Control and Decision Conference*, (San Antonio, Texas), December 1993.

[3] Z. Li and J. Canny, eds., *Nonholonomic Motion Planning.* Kluwer Academic Publishers, 1993.

[4] P. Jacobs and J. Canny, "Planning smooth paths for mobile robots," in *Nonholonomic Motion Planning* (Z. Li and J. Canny, eds.), ch. 8, Kluwer Academic Publishers, 1993.

[5] J. Laumond, "Nonholonomic motion planning versus controllability via the multibody car system example," Tech. Rep. STAN-CD 90-1345, Stanford University, 1990.

[6] J.-P. Laumond, "Singularities and topological aspects in nonholonomic motion planning," in *Nonholonomic Motion Planning* (Z. Li and J. Canny, eds.), ch. 5, Kluwer Academic Publishers, 1993.

[7] J.-P. Laumond, P. Jacobs, M. Taix, and R. M. Murray, "A motion planner for nonholonomic mobile robots," *IEEE Transactions on Robotics and Automation*, 1993. In press. Also available as LAAS technical report 90318, September 1990.

[8] J.-C. Latombe, *Robot Motion Planning.* Kluwer Academic Publishers, 1991.

[9] J. A. Reeds and L. A. Shepp, "Optimal paths for a car that goes both forwards and backwards," *Pacific Journal of Mathematics*, vol. 145, no. 2, pp. 367–393, 1990.

[10] L. Dubins, "On curves of minimal length with a constraint on average curvature, and with prescribed initial and terminal positions and tangents," *American Journal of Mathematics*, vol. 79, pp. 497–516, 1957.

[11] M. Secor, A. Sahai, and L. Bushnell, "An interactive steering software package for the SiliconGraphics workstation," Tech. Rep. UCB/ERL, University of California at Berkeley, 1994. (in preparation).

[12] L. Bushnell, D. Tilbury, and S. Sastry, "Steering three-input chained form nonholonomic systems using sinusoids: The fire truck example," in *Proceedings of the European Control Conference*, (Groningen, The Netherlands), pp. 1432–1437, June 1993.

[13] D. Tilbury, O. Sørdalen, L. Bushnell, and S. Sastry, "A multi-steering trailer system: Conversion into chained form using dynamic feedback," Tech. Rep. UCB/ERL M93/55, University of California at Berkeley, 1993.

[14] L. Bushnell, D. Tilbury, and S. Sastry, "Extended Goursat normal forms with applications to nonholonomic motion planning," in *Proceedings of the IEEE Control and Decision Conference*, (San Antonio, Texas), December 1993.